Wedge-Shaped Molecules with a Sulfonate Group at the Tip—A New Class of Self-Assembling Amphiphiles

Xiaomin Zhu,[a] Bernd Tartsch,[b] Uwe Beginn,*[a] and Martin Möller*[a]

Abstract: The synthesis of 4-*N*-[3′,4′,5′-tris(dodecyloxy)benzamido]benzene-4-sulfonic acid (**1**) and 4′-[3″,4″,5″-tris-(dodecyloxy)benzoyloxy]azobenzene-4-sulfonic acid (**2**) is described. Pure acid **1** is stable, while **2** can be stored only in solution. Both acids were obtained from their sodium salts and were quantitatively transformed into the pyridinium salts. The phase behavior of these acids, as well as the sulfonates was investigated by differential scanning calorimetry and polarizing optical microscopy. The investigated compounds exhibit columnar mesophases. The formation of columnar superstructures was demonstrated for the sodium sulfonates by scanning force microscopy, gelation experiments, and proton magnetic resonance spectroscopy.

Keywords: amphiphiles · mesophases · self-assembly · sulfonic acids

Introduction

Supramolecular chemistry based on weak, noncovalent interactions such as hydrogen bonding, as well as ionic interaction is a new and exciting branch of modern science. On one hand, it opens a way to discover the secret of nature, since numerous finite biological structures assemble themselves from their molecular components through non-covalent interactions; for example, collagen filaments, microtubuli, ribosomes, multienzyme complexes, cell membranes, and viruses..[1] On the other hand, self-assembly of small molecules into supramolecular organizations provides a novel approach towards complex aggregate architectures,[2] and offers exciting perspectives for the development of nanostructured functional materials.[3]

As is well known from the literature, wedge-shaped amphiphilic molecules that contain a polar head at the tip of the wedge and a large nonpolar body can self-assemble into well-defined rod-like structures.[4] Polymers that bear wedge-shaped side groups have also been synthesized and investigated,[5] and indeed, such monodendron-jacketed polymers have been shown to form columnar structures. In contrast to comblike molecules that contain flexible linear side chains, the formation of a cylindrical structure is predominately driven by the self-assembly of the side groups and not by the excluded volume effects of the side chains.[6] It has also been found that self-assembly of the wedge-shaped side groups into a cylindrical shape induces a disordered helical conformation of the flexible polymer chain located in the centre of the column. Such macromolecules have sufficiently thick diameters that single molecules can be directly visualized and quantitative analyzed in two dimensions by scanning force microscopy (SFM),[5] and in three dimensions by transmission electron microscopy (TEM).[7]

Now, if we replace the covalent bonds between the side groups and the backbone in the monodendron-jacketed polymers with weak bonds, such as ionic interactions and hydrogen bonds, these systems can be classified as physically bonded polymer–surfactant or polymer–amphiphile supramolecules. Such systems, which are readily microphase separated, represent a new class of materials that exhibit very interesting properties.[8] Some intractable rigid polymers like polyaniline can be rendered soluble or fusible with an alkyl-containing surfactant that has a reduced glass transition temperature. A large number of mesogenic and nonmesogenic amphiphilic surfactants have been used to complex polymer chains.[9] However, to the best of our knowledge, a report on wedge-shaped amphiphile–polymer systems has never been published.

The aim of the present work is to synthesize wedge-shaped molecules with a sulfonic acid group at the focal point (see Scheme 1) that can subsequently complex, through ionic interactions, polymer chains that contain complementary basic groups. This strategy should allow direct

[a] Dr. X. Zhu, Dr. U. Beginn, Prof. Dr. M. Möller
Institut für Technische Chemie und Makromolekulare Chemie
Lehrstuhl für Textilchemie und Makromolekulare Chemie der RWTH Aachen
Worringerweg 1, 52056 Aachen (Germany)
Fax: (+49) 241-80-22185
E-mail: uwe.beginn@texmc.rwth-aachen.de
moeller@dwi.rwth-aachen.de

[b] B. Tartsch
Abteilung Organische Chemie III/Makromolekulare Chemie
Universität Ulm
Albert-Einstein-Allee 11, 89069 Ulm (Germany)

 DOI: 10.1002/chem.200400050

visualization of the self-assembled individual supramolecular complexes. Furthermore, we will mimic the architecture of a tobacco mosaic virus, in which the central helical RNA chain is surrounded by 2130 "protein bricks" that make up the virus shell. In this structure the length of the virus is controlled by the length of the central macromolecule. In our example the natural protein building blocks are replaced by low molecular weight wedge-shaped molecules, and the RNA is substituted by a synthetic macromolecular chain.

Results and Discussion

The targeted general chemical structure of wedge-shaped sulfonic acid molecules is schematically depicted in Scheme 1. As direct sulfonation of 1,2,3-tris(alkoxy)benzene yields 2,3,4-tris(alkoxy)benzenesulfonic acid,[10] we decided to fix the sulfonic acid moiety by means of an aromatic functional link to a tris(alkoxy) benzoic acid fragment. Herein we describe the synthesis and characterization of two sulfonic acids, namely 4-*N*-[3′,4′,5′-tris(dodecyloxy)benzamido]benzene-4-sulfonic acid (**1**) and 4′-[3″,4″,5″-tris(dodecyloxy)benzoyloxy]azobenzene-4-sulfonic acid (**2**) (Scheme 2). In compound **1** the benzenesulfonic acid group was joined to the nonpolar fragment by an amide linkage, as amide groups form relatively strong hydrogen bonds, and therefore, may enhance the self-assembling properties of the amphiphiles. Meanwhile, compound **2** contains an extended aromatic azo fragment, which may also favor self-organization as a result of π stacking. Furthermore, the azo chromophore will allow us to follow the self-assembling process by absorbance bands shift, and to control this process by photoisomerization.

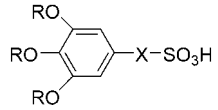

Scheme 1. General chemical structure of targeted wedge-shaped sulfonic acid molecules (R = $C_{12}H_{25}$–, **1**: X = –CONH–Ph-, **2**: X = –COO–Ph–N=N–Ph–).

The wedge-shaped sulfonic acids (**1**, **2**) were prepared according to the procedure illustrated in Scheme 2. Sodium *p*-aminobenzenesulfonate hydrate or sodium 4′-hydroxyazobenzenesulfonate in DMF were allowed to react in the presence of triethylamine with 3,4,5-tris(dodecyloxy)benzoyl chloride in dry THF. The reaction mixture was then poured into water, acidified, and extracted with chloroform. The products were purified by gradient columnar chromatography using THF/ethanol, and were freeze-dried from benzene. The resultant sodium sulfonates (**1**-Na, **2**-Na) were mixed with diisopropyl ether and stirred with Amberlyst 15 ion-exchange resin to obtain the corresponding sulfonic acids **1** and **2**. Interestingly, **1**-Na was soluble in diisopropyl ether, but after being stirred with ion-exchange resin compound **1** precipitated. In the case of **2**-Na and **2**, the opposite was observed, that is, **2**-Na was insoluble in diisopropyl ether, whereas **2** was soluble. The observed change in solubility is a good indication that the sulfonic acids are being formed. Subsequently, each sulfonic acid was quantitatively transformed into its pyridinium salt.

Sulfonic acid **1** was isolated as a white powder. Compound **2**, however, completely decomposed upon drying, but could be stored in solution for a considerable period of time (> half a year). Compound **1** is a crystalline compound at ambient temperature that melts into a liquid crystalline

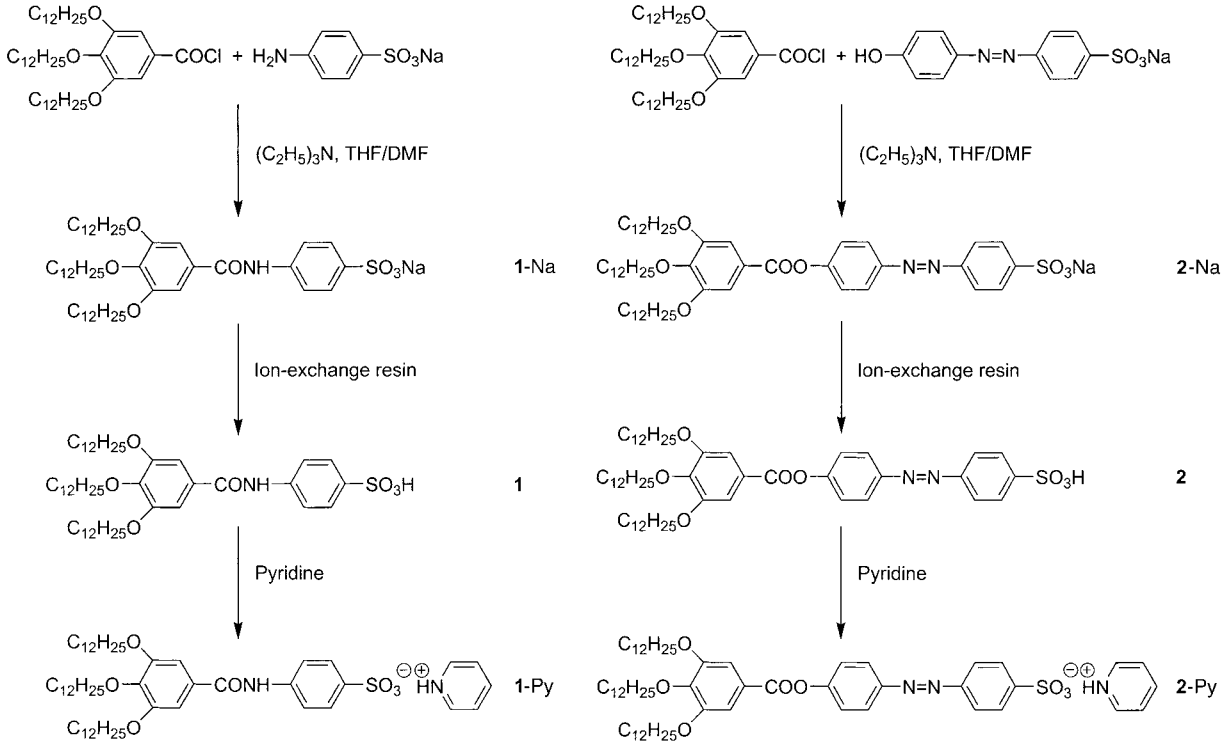

Scheme 2. Synthetic scheme for the preparation of the investigated amphiphilic sulfonates.

phase at 119 °C. The fan-shaped texture obtained upon cooling the sample from the isotropic melt is shown in Figure 1 A. This texture is typical for columnar mesophases. The transition temperatures determined by differential scanning calorimetry (DSC) in combination with polarizing optical microscopy (POM) are listed in Table 1.

The phase behavior of the sodium and pyridinium salts of these sulfonic acids has also been studied. The results of DSC and POM investigation are shown in Table 1. All the salts except compound **1**-Py, which forms an uncharacteristic liquid crystalline texture (Figure 1 B), form columnar mesophases. The fan-shaped texture typical for columnar mesophases for compound **2**-Py is shown in Figure 1 C.

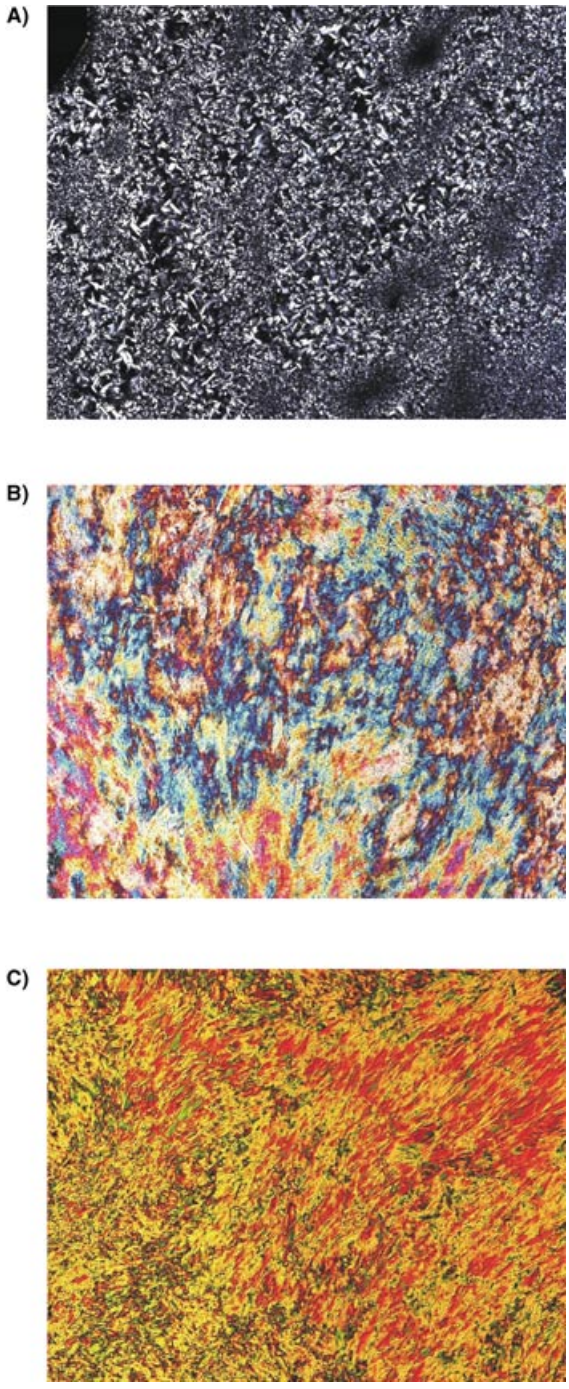

Figure 1. Optical micrographs of compounds **1**, **1**-Py, and **2**-Py between crossed polarizers: A) liquid crystalline texture of **1** obtained from the isotropic melt by cooling to 105 °C; B) liquid crystalline texture of **1**-Py at 67 °C; C) liquid crystalline texture of **2**-Py at 195 °C (Magnification 100×).

Table 1. Transition temperatures of compounds **1**, **1**-Py, **1**-Na, **2**-Py, and **2**-Na.

	$T_{C\rightarrow M}$[a] [°C]	$\Delta H_{C\rightarrow M}$[b] [kJ mol^{-1}]	$T_{M\rightarrow I}$[c] [°C]	$\Delta H_{M\rightarrow I}$[d] [kJ mol^{-1}]
1	119.0	101.3	132.0	< 0.1
1-Py	38.7	23.8	65.0	18.1
1-Na	60.0	56.1	> 300	–
2-Py	94.3	63.5	200[e]	–
2-Na	–	–	> 300	–

[a] $T_{C\rightarrow M}$ = melting temperature. [b] $\Delta H_{C\rightarrow M}$ = melting enthalpy. [c] $T_{M\rightarrow I}$ = isotropization temperature. [d] $\Delta H_{M\rightarrow I}$ = isotropization enthalpy. [e] With decomposition.

Although the sodium salts of these sulfonic acids (**1**-Na and **2**-Na) decomposed at very high temperatures [decomposition temperature is 330 °C as measured by thermogravimetric analysis (TGA)], they were below the isotropization temperatures. The presence of a mesophase was proven by applying pressure to the powders while they were between two glass plates, as the compounds sintered and gave a translucent mesoglass. A birefringent, but uncharacteristic texture was observed using a polarizing microscope.

The compounds were precipitated from ethanol to obtain a crystalline bulk structure. A sharp endothermic peak was observed in the DSC thermogram during the first heating run of the ethanol-precipitated **1**-Na. This peak, with a maximum at 60 °C and a transition enthalpy of $\Delta H =$ 56.1 kJ mol^{-1}, corresponds to the crystalline–liquid crystalline transition. However, only a couple of very broad endothermic signals were observed on the DSC curves of the ethanol-precipitated **2**-Na. This behavior is possibly the result of incomplete crystallization upon rapid precipitation.

One can see from Table 1 that the pyridinium salt **1**-Py exhibits a much lower transition temperature than the corresponding sulfonic acid **1**, while the isotropization point of the pure sodium salt **1**-Na exceeds both of the abovementioned ones, and is even higher than its decomposition temperature. Similarly, the isotropization temperature of **2**-Na is much higher than that of **2**-Py. Hence the sodium salts exhibit the widest mesophase temperature interval. A detailed structure investigation of all these compounds by wide and small-angle X-ray scattering is in progress.

It is well known that the presence of small amounts of inert impurities reduces the transition temperature of liquid crystalline phases without altering the mesophase type.[11] An attempt was made to reduce the transition temperatures of **1**-Na and **2**-Na so that they would be observable by mixing them with an inert organic solvent. The phase behaviour of the sodium sulfonates in the high boiling point organic solvent tetra(ethylene glycol) bis(2-ethylhexanoate) (TEGBEH) was studied. The solvent not only decreased the transition temperatures, but also reduced the melt viscosity, thereby allowing characteristic liquid crystalline textures to be formed (Figure 2). Compound **1**-Na formed a mosaic-like

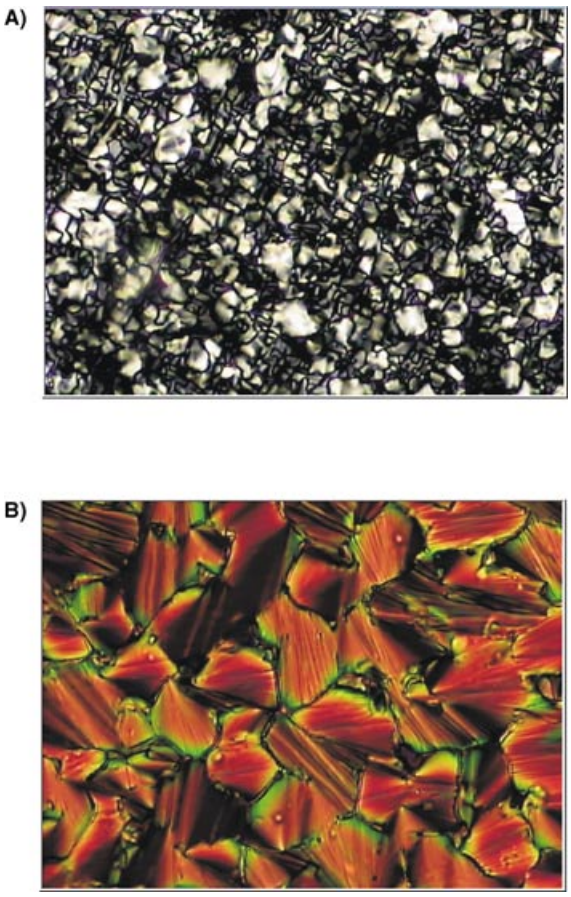

Figure 2. Liquid crystalline textures formed by sodium sulfonates **1**-Na and **2**-Na in tetra(ethylene glycol) bis(2-ethylhexanoate) (TEGBEH): A) 49 wt% of **1**-Na at 80°C; and B) 33 wt% of **2**-Na at 80°C (Magnification 100×).

texture (Figure 2A), while **2**-Na exhibited a fan-shaped texture (Figure 2B). Both of these textures are typical for columnar mesophases. The melting and isotropization transitions of **1**-Na and **2**-Na were detected in mixtures that contained as little as 10 wt% of the solute. As all the mixtures under investigation are easily supercooled, they were annealed at 50°C for 12–24 h before DSC measurement, and the transition temperatures were obtained from the first heating run (Figure 3).

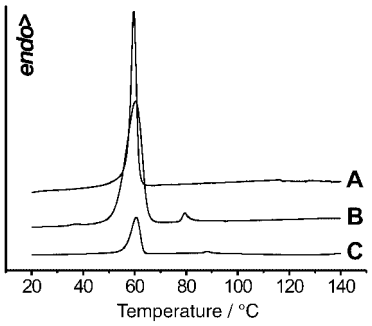

Figure 3. Representative DSC traces of **1**-Na and its mixtures with TEGBEH: A) Pure **1**-Na; B) 68 wt% of **1**-Na; and C) 25 wt% of **1**-Na (Data were obtained from the first heating run with a heating rate of 10 K min^{-1}).

The binary phase diagrams of **1**-Na and **2**-Na with TEGBEH were determined, and are depicted in Figure 4.

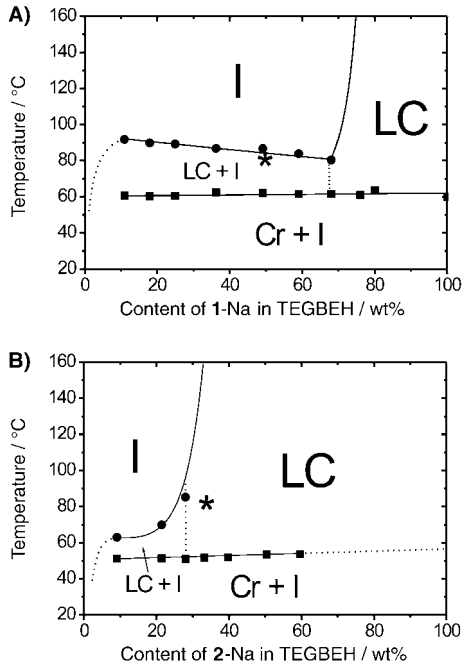

Figure 4. Phase diagrams of sodium sulfonates **1**-Na and **2**-Na in TEGBEH (*: conditions for texture micrographs in Figure 2).

The organic solvent barely affected the crystalline–liquid crystalline transition temperatures of these compounds, but the isotropization temperatures were drastically decreased. For the **1**-Na/TEGBEH mixtures, the isotropization temperature exceeded the decomposition temperature of TEGBEH ($T_d = 260$°C) up to a solvent content of 30 wt%. At higher solvent content the isotropization temperature was found to be between 80 (~30 wt% TEGBEH) and 92°C (~90 wt% TEGBEH). The small change in temperature relative to concentration ($dT_{iso}/dC_{TEGBEH} \approx 0.2$ K wt%) indicates the presence of a miscibility gap, that is, that the solvent saturated mesophase of **1**-Na separated from the TEGBEH phase. A similar phenomenon has been found to occur in mixtures of methacrylates and methacrylate-functionalized columnar crown ether amphiphiles.[12] In the region in which the isotropization temperature was weakly dependent upon concentration, a macrophase separation was observed (Figure 2A, Figure 4A), while in the region in which the solvent content was lower ($C_{TEGBEH} < 67$ wt%), polarizing microscopy showed the whole sample to exhibit a uniform texture (Figure 2B, Figure 4B). From the phase diagrams it was deduced that the columnar mesophase of **2**-Na can contain up to approximately 70 wt% of solvent, while for **1**-Na only 40 wt% can be present.

Self-assembly of the wedge-shaped sulfonate molecules can be visualized by means of SFM. Figure 5 depicts the tapping mode micrograph of a monolayer of **2**-Na which was spin-cast onto highly ordered, pyrolytic graphite (HOPG) at ambient temperature from chloroform solution (0.1 wt%). The densely packed, elongated rods are clearly observable.

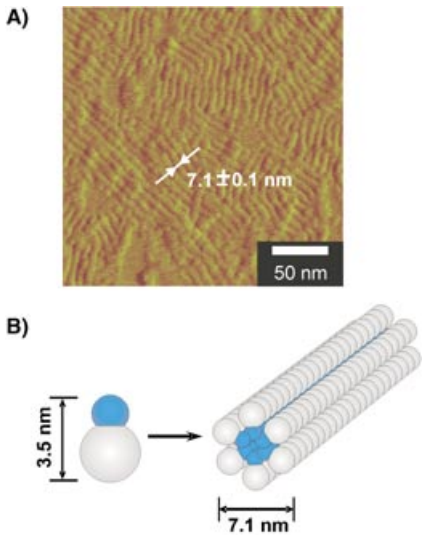

Figure 5. A) Tapping mode SFM micrograph (phase signal) of compound **2**-Na deposited on highly ordered pyrolytic graphite (HOPG); and B) the proposed packing model. The sample was prepared from chloroform solution (0.1 g L^{-1}) at ambient temperature by spin-casting at 2000 rpm.

The diameter of a single rod is (7.1 ± 0.1 nm). As the length of a molecule of **2**-Na was estimated to be 3.5 nm from space-filling models (assuming stretched alkyl chains), a head-to-head arrangement without overlap of the head group is proposed.

It is well known that loss of molecular mobility caused by aggregation is reflected by an increase in line width. As a result, NMR spectroscopy indicated that these amphiphilic sulfonates display different association properties in different organic solvents. Figure 6 depicts the ^{1}H NMR spectra of compounds **1**-Na and **2**-Na in $CDCl_3$ and [D_6]DMSO. The

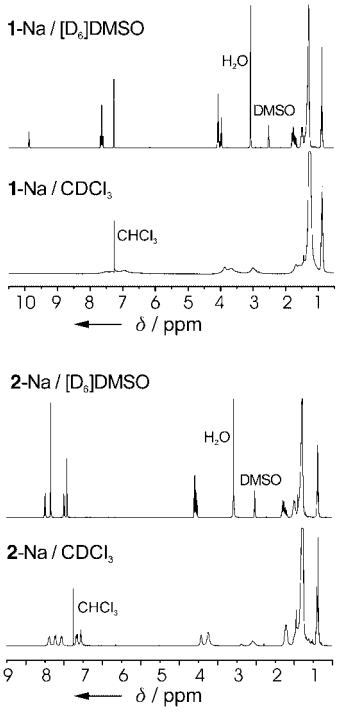

Figure 6. ^{1}H NMR spectra of **1**-Na and **2**-Na in $CDCl_3$ at ambient temperature, and [D_6]DMSO at 80 °C.

^{1}H NMR resonance signals in $CDCl_3$ solution, especially those close to the tip of the wedge, are similar to those displayed by polymeric substrates, that is, they are broad. Signals arising from the alkyl parts were only slightly affected; this indicates that they are conformationally mobile. On the other hand, the signals in DMSO were all sharp and well separated, and displayed the expected hyperfine structure. These results indicate that the wedge-shaped amphiphilic molecules self-assemble into rod-like structures in dilute solutions with non-polar solvents because there is a hydrophobic–hydrophilic balance between the polar tip and the non-polar bulk of the molecular wedges. An increase in concentration or a decrease in temperature leads to the entanglement of the rods, and as a result gelation occurs. Aggregation was not observed in solutions with highly polar solvents.

As the signals in ^{1}H NMR spectra of the pyridinium salts in $CDCl_3$ were sharp, molecular association does not occur in **1**-Py and **2**-Py. This corresponds to the results obtained during gelation experiments, which determined that neither compound has good gelation properties.

The formation of isolated columnar superstructures can be deduced from the gelation properties displayed by the amphiphiles in organic solvents, as formation of rodlike associations will cause thermoreversible gelation even at low concentrations.[13] Although all the compounds synthesized in this work form liquid crystalline phases, only the sodium salts of sulfonic acids **1**-Na and **2**-Na are gelators. The gelation experiments were carried out by two different methods. The first involved heating a mixture of the solute and solvent until a clear solution was obtained, and this was then slowly cooled to ambient temperature. In the second approach, the hot solution was shock frozen by liquid nitrogen and then slowly warmed to ambient temperature. Qualitative gelation test results for solutions of **1**-Na and **2**-Na in various organic solvents of different polarity are summarized in Table 2. Phase separation, that is, white gel formation and precipitation, was observed in polar solvents like ethanol, DMF, and DMSO, while transparent or translucent gels were formed in nonpolar solvents. Moreover, the gelation ability of sulfonic acid **2**-Na, which contains a longer aromatic fragment, is higher than that of **1**-Na. As shown in our previous work,[14] white gels consist of relatively large, irregular shaped clusters of small needlelike aggregates, whereas transparent gels contain well defined supramolecular cylinders that are homogeneously dispersed. In Figure 7 one can see small crystals of **2**-Na dispersed in the white gel formed by 5 wt % **2**-Na in butylacetate. A network of well defined fibers formed by **2**-Na in *n*-hexane was observed by means of tapping mode SFM (Figure 8). The width of the thinnest fibers was found to be less than 10 nm; this roughly corresponds to twice the length of one individual molecule (ca. 7 nm).

Conclusion

The wedge-shaped amphiphiles **1** and **2**, both of which contain a sulfonic acid group at their focal points, as well as

Table 2. Gel formation of sodium sulfonates **1**-Na and **2**-Na in 5 wt% solutions.

Solvent	**1**-Na	**2**-Na
ethanol	white gel at ambient temperature	precipitate at ambient temperature
DMSO	precipitate at ambient temperature	precipitate at ambient temperature
DMF	white gel at ambient temperature	precipitate at ambient temperature
THF	translucent gel at 4 °C	translucent gel at 4 °C
chloroform	translucent gel at 4 °C	transparent gel at 4 °C
butylacetate	precipitate at ambient temperature	white gel at ambient temperature
toluene	solution at −20 °C	viscous liquid at ambient temperature, a translucent gel was formed at −20 °C
n-hexane	solution at −20 °C	transparent gel upon being stored at −20 °C for 1 week, the gel does not melt upon warming to ambient temperature

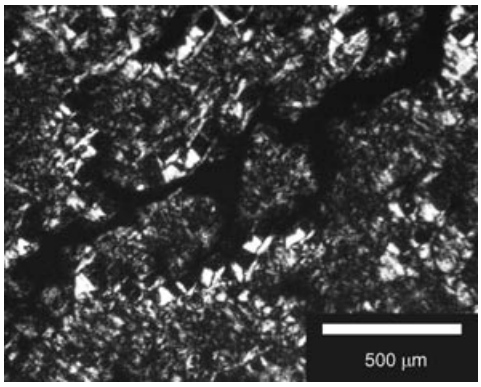

Figure 7. Polarizing optical micrograph of a white gel formed by 5 wt% of **2**-Na in butylacetate.

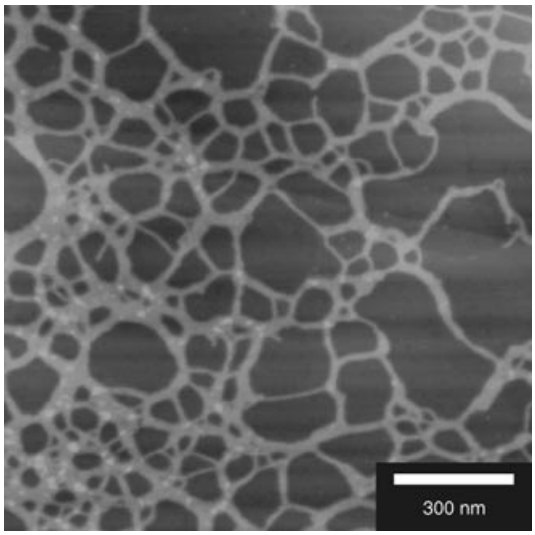

Figure 8. Tapping mode SFM micrograph (height signal) of compound **2**-Na on highly ordered pyrolytic graphite (HOPG). The sample was prepared from *n*-hexane solution (0.5 g L^{-1}) at ambient temperature by spin-casting at 2000 rpm.

their sodium and pyridinium salts were synthesized for the first time. It was demonstrated that with the exception of **1**-Py all investigated compounds exhibited columnar mesophases. The most stable mesophases were observed for the sodium salts **1**-Na and **2**-Na. The formation of columnar superstructures was proven by SFM and gelation tests. Phase diagram investigations demonstrate that the transition from gel state to highly ordered bulk phase occurs through a lyotropic mesomorphism that bridges the gap between the two singular organized states (gel⇌bulk phases).

The wedge-shaped sulfonate molecules are also of interest for the preparation of functional materials because as they assemble into solid supramolecular columns, the sulfonate groups stack along the cylinder axis, thus forming a potential transport channel. If such columns are embedded and covalently linked into a polymer matrix, the corresponding films may serve as a new type of ion-selective membrane.[15]

Future work will focus on such materials as well as on the complexes that are formed between the wedge-shaped sulfonic acid molecules and polybases such as poly(2-vinylpyridine), poly(4-vinylpyridine) or conductive polymers like polyaniline and polypyridine.

Experimental Section

Techniques: A Zeiss AXIOSKOP polarizing microscope equipped with a Mettler FP 82 hot stage and a photoautomat Mettler FP 80 was used for thermo-optical analyses. DSC measurements were performed using a Perkin-Elmer DSC 7 unit. Samples (typical weight: 5 mg) were enclosed in standard Perkin-Elmer 30 μL/0.15 aluminum pans. Indium and zinc were used as calibration standards. Heating and cooling rates were 10 °C min^{-1}. As all the samples could easily be supercooled, the phase transition data were obtained from the first heating run. Infrared spectra were taken on a Bruker IFS 66 V-Spectrophotometer. ^{1}H NMR (300 MHz) and ^{13}C NMR (75 MHz) spectra were recorded on a Bruker DPX 300 spectrometer using tetramethylsilane (TMS) as an internal standard. UV/Vis spectra were recorded on a Perkin Elmer Lambda 16 UV-vis spectrometer. Thin-layer chromatography (TLC) was performed on Merck KG-60/F254 TLC plates and detected with UV light (254 nm) or with iodine vapour. Elemental analyses for **1**-Na and **2**-Na were performed by the microanalytical laboratory of A. N. Nesmeyanov Institute of Organoelement Compounds of the Russian Academy of Sciences, while all other compounds were analyzed with a Carlo Erba MOD 1106 instrument. A Nanoscope III (Digital Instruments, St. Barbara) operating in the tapping mode at a resonance frequency of 360 kHz was used for SFM. The measurements were performed at ambient conditions using silicon probes with a spring constant of 150 N m^{-1}.

Materials: Methyl 3,4,5-trihydroxybenzoate (98%, Aldrich), 1-bromododecane (97%, Aldrich), sulfanilic acid (99%, Aldrich), sulfanilic acid sodium salt hydrate (97%, Aldrich), thionyl chloride (99+%, Aldrich), triethylamine (p.a. grade, Merck), potassium carbonate (99%, Merck), Amberlyst 15 ion-exchange resin (Aldrich), pyridine (99+%, Aldrich), cyclohexanone (z. S., Merck), phenol (p.a. grade, Merck), and sodium nitrite (97+%, Aldrich) were used as received. p.a. grade organic solvents from Merck were used for the gelation experiments. Tetrahydrofuran (THF), *N*,*N*-dimethylformamide (DMF), dimethyl sulfoxide (DMSO),

ethanol, chloroform, diethyl ether, diisopropyl ether, benzene, sodium sulphate, sodium hydrogen carbonate and sodium hydroxide were gifts from the "Fonds der Chemischen Industrie", and were purified according to standard procedures. Sodium 4′-hydroxyazobenzenesulfonate was synthesized according to a standard coupling procedure.[16] 3,4,5-Tris(dodecyloxy)benzoyl chloride was also prepared as described in the literature.[17]

Syntheses

Sodium {4-*N*-[3′,4′,5′-tris(dodecyloxy)benzamido]benzene-4-sulfonate} (1-Na): To a well stirred solution of sulfanilic acid sodium salt hydrate (0.7 g, 3.6 mmol) and triethylamine (0.5 mL, 3.6 mmol) in DMF (20 mL) at 0 °C was slowly added a solution of 3,4,5-tris(dodecyloxy)benzoyl chloride (2.0 g, 2.9 mmol) in dried THF (20 mL). Upon complete addition stirring was continued for 12 h. The reaction mixture was poured into water (400 mL), acidified to a pH of 3, and was then extracted several times with chloroform. The extract was dried with sodium sulfate, and the solvent was removed under reduced pressure. The product was purified by gradient columnar chromatography using THF/ethanol. THF was firstly used to wash away all the impurities, and then the product was washed out using a mixture THF/ethanol (1:5). The purified product was dissolved in dried benzene to give a 10 wt% solution, and this was filtered through a membrane filter with a pore size of 5 μm. A white powder was obtained after the filtrate was freeze-dried. Yield: 1.85 g (75%), purity >98% by ^{1}H NMR spectroscopy. ^{1}H NMR (300 MHz, [D$_6$]DMSO, 80 °C, TMS): δ = 0.88 (t, 9H; CH_3), 1.28 (m, 48H; $(CH_2)_8CH_3$), 1.48 (m, 6H; $CH_2(CH_2)_2OPh$), 1.70 (m, 2H; CH_2CH_2OPh in 4′ position relative to CO group), 1.77 (m, 4H; CH_2CH_2OPh in 3′,5′ position relative to CO group), 3.97 (t, ^3J(H,H) = 6.4 Hz, 2H; CH_2OPh in 4′ position relative to CO group), 4.07 (t, ^3J(H,H) = 6.2 Hz, 4H; CH_2OPh in 3′,5′ position relative to CO group), 7.28 (s, 2H; ArH *ortho* to CO group), 7.62 (d, ^3J(H,H) = 9.0 Hz, 2H; ArH *meta* to SO_3Na group), 7.68 (d, ^3J(H,H) = 8.7 Hz, 2H; ArH *ortho* to SO_3Na group), 9.89 ppm (s, 1H; PhCONHPh); ^{13}C NMR (75 MHz, [D$_6$]DMSO, 80 °C, TMS): δ = 14.02 (CH_3), 22.30 (CH_2CH_3), 25.90 ($CH_2(CH_2)_2OPh$), 25.95–31.57 (alkyl), 69.46 (CH_2OPh in 3′,5′ position relative to CO group), 73.01 (CH_2OPh in 4 position relative to CO group), 107.47 (ArC *ortho* to CO group), 120.01 (ArC *meta* to SO_3Na group), 126.33 (ArC *ortho* to SO_3Na group), 130.03 (ArC *ipso* to CO group), 139.42 (ArC *ispo* to SO_3Na group), 141.36 (ArC in 4′ position relative to CO group), 144.57 (ArC *ipso* to NH group), 152.74 (ArC in 3′,5′ position relative to CO group), 165.19 ppm (PhCONHPh); IR (KBr): $\tilde{\nu}$ = 3432, 3265, 2956, 2919, 2850, 1646, 1587, 1528, 1500, 1468, 1427, 1386, 1343, 1241, 1123, 1045, 1013, 990, 830, 705, 664, 609, 566 cm^{-1}; elemental analysis calcd (%) for $C_{49}H_{82}O_7NSNa$ (852.3): C 69.05, H 9.70, N 1.64, S 3.76; found: C 67.20, H 9.34, N 1.56, S 3.55.

Sodium {4′-[3″,4″,5″-tris(dodecyloxy)benzoyloxy]azobenzene-4-sulfonate} (2-Na): Compound **2**-Na was prepared and isolated in the manner described for the synthesis of **1**-Na.. To a well stirred solution of sodium 4′-hydroxyazobenzenesulfonate (2.75 g, 9.2 mmol) and triethylamine (5 mL, 36 mmol) in DMF (50 mL) was added a solution of 3,4,5-tris(dodecyloxy)benzoyl chloride (5.13 g, 7.4 mmol) in dried THF (50 mL). An orange powder was obtained after the compound was freeze-dried from benzene. Yield: 4.2 g (60%), purity >98% by ^{1}H NMR spectroscopy. ^{1}H NMR (300 MHz, [D$_6$]DMSO, 80 °C, TMS): δ = 0.87 (t, 9H; CH_3), 1.27 (m, 48H; $(CH_2)_8CH_3$), 1.47 (m, 6H; $CH_2(CH_2)_2OPh$), 1.71 (m, 2H; CH_2CH_2OPh in 4′ position relative to CO group), 1.78 (m, 4H; CH_2CH_2OPh in 3′,5′ position relative to CO group), 4.04 (t, ^3J(H,H) = 6.4 Hz, 2H; CH_2OPh in 4′ position relative to CO group), 4.08 (t, ^3J(H,H) = 6.0 Hz, 4H; CH_2OPh in 3′,5′ position relative to CO group), 7.42 (s, 2H; ArH *ortho* to CO group), 7.50 (d, ^3J(H,H) = 8.7 Hz, 2H; ArH *ortho* to OCOPh group), 7.85 (s, 4H; ArH *ortho* and *meta* to SO_3Na group), 8.00 ppm (d, ^3J(H,H) = 8.7 Hz, 2H; ArH *meta* to OCOPh group); ^{13}C NMR (75 MHz, [D$_6$]DMSO, 80 °C, TMS): δ = 14.02 (CH_3), 22.30 (CH_2CH_3), 25.87 ($CH_2(CH_2)_2OPh$), 25.95–31.57 (alkyl), 69.55 (CH_2OPh in 3,5-dodecyl), 73.17 (CH_2OPh in 4-dodecyl), 109.39 (ArC *ortho* to CO group), 122.26 (ArC *ortho* to OCOPh group), 123.09 (ArC *meta* to OCOPh group), 124.09 (ArC *meta* to SO_3Py group), 127.12 (ArC *ortho* to SO_3Py group), 153.04 ppm (ArC in 3′,5′ position relative to CO group); IR (KBr): $\tilde{\nu}$ = 3437, 2923, 2853, 1734, 1663, 1591, 1500, 1467, 1432, 1388, 1339, 1198, 1125, 1043, 1009, 946, 848, 804, 747, 712, 671, 637, 575 cm^{-1}; UV/Vis (*n*-hexane): λ_{max} (ε) = 314.4 (28150), (chloroform): λ_{max} (ε) = 325.6 (19175), (DMF): λ_{max} (ε) = 336.0 nm (26587 mol^{-1} dm^3 cm^{-1}); elemental analysis calcd (%) for $C_{55}H_{85}O_8N_2SNa$ (957.4): C 69.00, H 8.95, N 2.93, S 3.35, Na 2.40; found: C 67.59, H 8.98, N 2.86, S 3.15, Na 2.30.

4-*N*-[3′,4′,5′-tris(dodecyloxy)benzamido]benzene-4-sulfonic acid (1): Compound **1**-Na (0.5 g, 0.59 mmol) was dissolved in dry diisopropyl ether (50 mL). The resultant solution was stirred overnight with ion-exchange resin (5 g, amberlyst 15), decanted, and the solvent was removed under reduced pressure. The product was dried under vacuum at 40 °C. Yield: 0.49 g (100%), purity >98% by ^{1}H NMR spectroscopy. ^{1}H NMR (300 MHz, [D$_6$]DMSO, 60 °C, TMS): δ = 0.81 (t, 9H; CH_3), 1.22 (m, 48H; $(CH_2)_8CH_3$), 1.43 (m, 6H; $CH_2(CH_2)_2OPh$), 1.64 (m, 2H; CH_2CH_2OPh in 4′ position relative to CO group), 1.71 (m, 4H; CH_2CH_2OPh in 3′,5′ position relative to CO group), 3.88 (t, ^3J(H,H) = 6.0 Hz, 2H; CH_2OPh in 4′ position relative to CO group), 4.00 (t, ^3J(H,H) = 5.7 Hz, 4H; CH_2OPh in 3′,5′ position relative to CO group), 7.24 (s, 2H; ArH *ortho* to CO group), 7.57 (d, ^3J(H,H) = 8.7 Hz, 2H; ArH *meta* to SO_3H group), 7.69 (d, ^3J(H,H) = 8.7 Hz, 2H; ArH *ortho* to SO_3H group), 10.10 ppm (s, 1H; PhCONHPh); IR (KBr): $\tilde{\nu}$ = 3436, 2921, 2851, 1640, 1620, 1596, 1525, 1502, 1468, 1429, 1399, 1340, 1241, 1209, 1174, 1120, 1038, 1011, 838, 706, 668 cm^{-1}; elemental analysis calcd (%) for $C_{49}H_{83}O_7NS$ (830.3): C 70.89, H 10.08, N 1.69; found: C 67.19, H 9.60, N 1.59.

Pyridinium {4-*N*-[3′,4′,5′-tris(dodecyloxy)benzamido]benzene-4-sulfonate} (1-Py): Compound **1** (0.2 g, 0.24 mmol) was suspended in chloroform (20 mL) and a solution of pyridine (20 mg, 0.25 mmol) in chloroform (20 mL) was added dropwise. The resultant mixture was stirred for an additional 2 h, and then the solvent was removed on under reduced pressure. The product was dried under vacuum at 40 °C. Yield: 0.22 g (100%), purity >98% by ^{1}H NMR spectroscopy. ^{1}H NMR (300 MHz, $CDCl_3$, 25 °C, TMS): δ = 0.87 (t, 9H; CH_3), 1.25 (m, 48H; $(CH_2)_8CH_3$), 1.43 (m, 6H; $CH_2(CH_2)_2OPh$), 1.74 (m, 6H; CH_2CH_2OPh), 3.98 (t, ^3J(H,H) = 6.0 Hz, 6H; CH_2OPh), 7.19 (s, 2H; ArH *ortho* to CO group), 7.66 (d, ^3J(H,H) = 8.9 Hz, 2H; ArH *meta* to SO_3Py group), 7.73 (d, ^3J(H,H) = 8.7 Hz, 2H; ArH *ortho* to SO_3Py group), 7.82 (t, ^3J(H,H) = 7.0 Hz, 2H; β-H of pyridine ring), 8.31 (t, ^3J(H,H) = 7.7 Hz, 2H; γ-H of pyridine ring), 8.76 (t, ^3J(H,H) = 5.3 Hz, 2H; α-H of pyridine ring), 8.95 ppm (s, 1H; PhCONHPh); ^{13}C NMR (75 MHz, $CDCl_3$, 25 °C, TMS): δ = 14.12 (CH_3), 22.70 (CH_2CH_3), 26.19 ($CH_2(CH_2)_2OPh$), 26.65–31.90 (alkyl), 69.25 (CH_2OPh in 3′,5′ position relative to CO group), 73.50 (CH_2OPh in 4 position relative to CO group), 105.98 (ArC *ortho* to CO group), 120.53 (ArC *meta* to SO_3Py group), 126.67 (ArC *ortho* to SO_3Py group), 127.12 (β-C of pyridine ring), 129.21 (ArC *ipso* to CO group), 139.96 (ArC *ipso* to SO_3Py group), 140.22 (α-C of pyridine ring), 141.22 (ArC in 4′ position relative to CO group), 141.78 (γ-C of pyridine ring), 146.84 (ArC *ipso* to NH group), 153.06 (ArC in 3′,5′ position relative to CO group), 165.94 ppm (PhCONHPh); IR (KBr): $\tilde{\nu}$ = 3311, 3068, 2956, 2920, 2851, 1649, 1596, 1582, 1527, 1501, 1488, 1468, 1427, 1398, 1387, 1340, 1311, 1260, 1235, 1172, 1116, 1034, 1009, 802, 764, 704, 687, 566 cm^{-1}; elemental analysis calcd (%) for $C_{54}H_{88}O_7N_2S$ (909.4): C 71.32, H 9.75, N 3.08; found: C: 67.58, H 9.72, N 2.99.

4′-[3″,4″,5″-tris(dodecyloxy)benzoyloxy]azobenzene-4-sulfonic acid (2) and pyridinium {4′-[3″,4″,5″-tris(dodecyloxy)benzoyloxy]azobenzene-4-sulfonate} (2-Py): Compound **2**-Na (0.2 g, 0.21 mmol) dispersed in dried diisopropyl ether (20 mL) was stirred overnight with ion-exchange resin (2 g, amberlyst 15). The resultant sulfonic acid could not be isolated in a dried state because of its instability. The solution was filtered through a glass filter (pore size = 4) and added dropwise to a well stirred solution of pyridine (20 mg, 0.25 mmol) in chloroform (20 mL). The resultant mixture was stirred for an additional 2 h, and the solvent was then removed under reduced pressure. The product was dried under vacuum at 40 °C. Yield: 0.22 g (100%), purity >98% by ^{1}H NMR spectroscopy. ^{1}H NMR (300 MHz, $CDCl_3$, 25 °C, TMS): δ = 0.88 (t, 9H; CH_3), 1.26 (m, 48H; $(CH_2)_8CH_3$), 1.50 (m, 6H; $CH_2(CH_2)_2OPh$), 1.77 (m, 2H; CH_2CH_2OPh in 4′ position relative to CO group), 1.84 (m, 4H; CH_2CH_2OPh in 3′,5′ position relative to CO group), 4.06 (t, ^3J(H,H) = 6.4 Hz, 2H; CH_2OPh in 4′ position relative to CO group), 4.07 (t, ^3J(H,H) = 6.4 Hz, 4H; CH_2OPh in 3′,5′ position relative to CO group), 7.37 (d, ^3J(H,H) = 8.9 Hz, 2H; ArH *ortho* to OCOPh group), 7.42 (s, 2H; ArH *ortho* to CO group), 7.95 (d, ^3J(H,H) = 8.7 Hz, 2H; ArH *ortho* to SO_3Py group), 7.99 (t, 2H; β-H of pyridine ring), 8.02 (d, ^3J(H,H) = 9.1 Hz, 2H; ArH *meta* to SO_3Py group), 8.12 (d, ^3J(H,H) = 8.7 Hz, 2H; ArH *meta* to OCOPh group), 8.45 (t, ^3J(H,H) = 7.7 Hz, 1H; γ-H of pyridine ring), 9.06 ppm (d, ^3J(H,H) = 5.3 Hz, 2H; α-H of pyridine ring); ^{13}C NMR (75 MHz, $CDCl_3$, 25 °C,

TMS): $\delta = 14.13$ (CH_3), 22.70 (CH_2CH_3), 26.10 ($CH_2(CH_2)_2OPh$), 25.95–31.95 (alkyl), 69.29 (CH_2OPh in 3,5-dodecyl), 73.62 (CH_2OPh in 4-dodecyl), 108.61 (ArC *ortho* to CO group), 122.56 (ArC *ortho* to OCOPh group), 122.86 (ArC *meta* to OCOPh group), 123.51 (ArC *ipso* to CO group), 124.34 (ArC *meta* to SO_3Py group), 127.13 (ArC *ortho* to SO_3Py group), 127.20 (β-C of pyridine ring), 142.22 (α-C of pyridine ring), 143.20 (ArC in 4′ position relative to CO group), 145.72 (ArC *ipso* to SO_3Py group), 146.66 (ArC *para* to OCOPh group), 150.16 (ArC *ipso* to OCOPh group), 153.02 (γ-C of pyridine ring), 153.25 (ArC in 3′,5′ position relative to CO group), 153.42 (ArC *para* to SO_3Py group), 164.73 ppm (PhCOOPh); IR (KBr): $\tilde{\nu} = 3069$, 2955, 2920, 2851, 1728, 1615, 1586, 1541, 1498, 1468, 1432, 1384, 1338, 1227, 1207, 1119, 1033, 1009, 945, 856, 762, 712, 690, 635, 573, 557 cm^{-1}; UV/Vis (chloroform): λ_{max} (ε) = 328.0 nm (19880 $mol^{-1} dm^3 cm^{-1}$); elemental analysis calcd (%) for $C_{60}H_{91}O_8N_3S$ (1014.5): C 70.35, H 9.27, N 4.14**;** found: C 71.04, H 9.04, N 4.14.

Acknowledgements

The financial support of the German Research Foundation, DFG (SFB 569-A6), and the Alexander von Humboldt Foundation is gratefully acknowledged.

[1] a) S. J. Martin, *The Biochemistry of Viruses*, Cambridge University Press, London, **1978**, p. 145; b) R. H. Garrett, C. M. Grisham, *Principles of Biochemistry with a Human Focus*, Harcourt College Publishers, New York, **2002**, p. 893.
[2] J.-M. Lehn, *Supramolecular Chemistry. Concepts and Perspectives*, VCH, Weinheim, **1995**, p. 266.
[3] a) *Molecular Self-Assembly, Organic Versus Inorganic Approaches in Structure and Bonding Vol. 96* (Eds.: M. Fujita), Springer, Berlin, **2000**, p. 254; b) T. Kato, *Science* **2002**, *295*, 2414–2418; c) L. Brunsveld, B. J. B. Folmer, E. W. Meijer, R. P. Sijbesma, *Chem. Rev.* **2001**, *101*, 4071–4098; d) P. Terech, R. G. Weiss, *Chem. Rev.* **1997**, *97*, 3133–3160.
[4] V. Percec, J. Heck, G. Johansson, D. Tomazos, G. Ungar, *Macromol. Symp.* **1994**, *77*, 237–265.
[5] V. Percec, C.-H. Ahn, G. Ungar, D. J. P. Yeardley, M. Möller, S. Sheiko, *Nature* **1998**, *391*, 161–164.
[6] N. A. Platé, V. P. Shibaev, *Comb-Shaped Polymers and Liquid Crystals*, Plenum Press, New York, **1987**, p. 303.
[7] S. D. Hudson, H.-T. Jung, V. Percec, W.-D. Cho, G. Johansson, G. Ungar, V. S. K. Balagurusamy, *Science* **1997**, *278*, 449–452.
[8] a) O. Ikkala, G. ten Brinke, *Science* **2002**, *295*, 2407–2409; b) J. Ruokolainen, R. Mäkinen, M. Torkkeli, R. Serimaa, T. Mäkelä, G. ten - Brinke, O. Ikkala, *Science* **1998**, *280*, 557–560; c) M. Antonietti, J. Conrad, A. Thünemann, *Macromolecules* **1994**, *27*, 6007–6011; c) G. H. Fredrickson, *Macromolecules* **1993**, *26*, 2825–2831.
[9] a) O. Ikkala, J. Ruokolainen, G. ten Brinke, M. Torkkeli, R. Serimaa, *Macromolecules* **1995**, *28*, 7088–7094; b) J. Ruokolainen, M. Torkkeli, R. Serimaa, E. Komanschek, G. ten Brinke, O. Ikkala, *Macromolecules* **1997**, *30*, 2002–2007; c) J. Ruokolainen, J. Tanner, G. ten Brinke, O. Ikkala, M. Torkkeli, R. Serimaa, *Macromolecules* **1995**, *28*, 7779–7784; d) M. Antonietti, A. Wenzel, A. Thünemann, *Langmuir* **1996**, *12*, 2111–2114; e) R. V. Tal'roze, S. A. Kuptsov, T. I. Sycheva, V. S. Bezborodov, Platé, N. A. , *Macromolecules* **1995**, *28*, 8689–8691; f) Y. Cao, P. Smith, A. J. Heeger, *Synth. Met.* **1992**, *48*, 91–97.
[10] G. Pifferi, R. Monguzzi, *J. Pharm. Sci.* **1973**, *62*, 1392–1394.
[11] H. Kelker, R. Hatz, *Ber. Bunsen-Ges.* **1974**, *78*, 819–834.
[12] U. Beginn, G. Zipp, M. Möller, *Chem. Eur. J.* **2000**, *6*, 2016–2023.
[13] A. P. Philipse, *Langmuir* **1996**, *12*, 1127–1133.
[14] U. Beginn, G. Zipp, M. Möller, *J. Polym. Sci. A: Polym. Chem.* **2000**, *38*, 631–640.
[15] U. Beginn, *Adv. Mater.* **1998**, *10*, 1391–1394.
[16] L. R. Whitlock, S. Siggia, J. E. Smola, *Anal. Chem.* **1972**, *44*, 532–536.
[17] J. Malthete, A.-M. Levelut, N. Huu Tinh, *J. Phys. Lett.* **1985**, *46*, L875–880.

Received: January 16, 2004
Published online: June 24, 2004

